In vitro mechanisms of chlorophyllin antimutagenesis against dibenzo[*a*,*l*]pyrene

An Undergraduate Thesis in Bioresource Research

Oregon State University

Marita C. Barth

June 3, 1998

Approved June 17, 1998

George A Bailey

Thesis Supervisor

Introduction

Polycyclic aromatic hydrocarbons (PAHs) are a class of usually planar compounds consisting of fused aromatic rings that are formed by the incomplete combustion of organic materials. PAHs are ubiquitous in the environment, coming from a number of sources, such as cigarette smoke, the burning of wood for residential heating, and combustion of fossil fuels in automobiles and in industrial processes.

Human exposure to PAHs, through inhalation and ingestion, is attributable to a number of sources. Automobile exhaust, cigarette smoke, industrial emissions and smoke from wood burning are all potential sources of inhalation exposure. Particulates from these airborne sources are deposited on soil and water, and as a result exposure may occur through ingestion of contaminated water and food. Processing or preparing foods by pyrolytic methods such as barbecuing and smoking also results in elevated PAH content. There is also risk of occupational exposure to PAHs for workers in industries such as coal tar production and municipal incineration where carbonaceous materials are burned.

While there is some danger of acute toxicity from certain PAHs at high doses, the primary health concern is due to the carcinogenic nature of some of the compounds at lower doses. Although many of the lower molecular weight compounds are not carcinogenic, at least 15 PAHs have been shown to induce tumors in laboratory animals, including (7,12)dimethylbenz[*a*]anthracene (DMBA), benzo[*a*]pyrene (B[*a*]P) and dibenzo[*a,l*]pyrene (DB[*a,l*]P)[1]. This tumorigenic activity is a result of metabolic activation of the PAHs by cytochrome P-450 enzymes.

Cytochrome P-450 enzymes are a superfamily of inducible phase I metabolic enzymes which chemically modify a diverse array of endogenous and exogenous chemicals. While in many cases the modification of xenobiotic compounds decreases toxicity, it can also lead to an increase in toxicity. Such increases in toxicity can include the activation of procarcinogens to their reactive forms.

The major pathway of PAH activation is proposed to be conversion to diol-epoxide metabolites by the CYP1A family of cytochrome P-450 enzymes. (Fig. 1) An initial CYP1A-mediated monooxygenation results in an epoxide that is hydrolyzed to a dihydrodiol by epoxide hydrolase. A subsequent CYP1A monooxygenation converts the compound to the ultimately carcinogenic diol-epoxide form.

The orientation of the epoxide on the PAH molecule is key to the carcinogenic potency of the metabolite. According to the bay-region theory proposed by Jerina and Lehr,[2] the most reactive metabolite will be that with an epoxide on a saturated angular benzylic ring, forming part of a "bay-region". This hypothesis has been supported by studies with various PAHs including B[*a*]P[3] and benz[*a*]anthracene (B[*a*]A).[4]

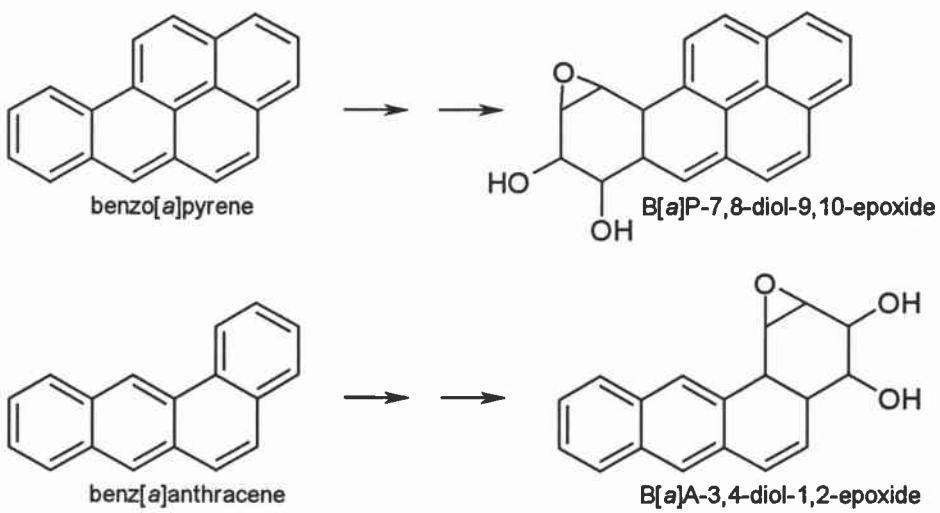

Figure 1: Examples of PAHs and their bay-region diol-epoxide metabolites

Dibenzo[*a,l*]pyrene is a PAH that has been isolated from cigarette smoke condensate [5] and is also present in fossil fuels and coal gasification products.[1] The significance of DB[*a,*l]P as an environmental carcinogen has only recently been appreciated. Earlier tumorigenicity tests using the weakly active dibenzo[*a,e*]fluor-anthrene had been erroneously attributed to DB[*a,l*]P.[6,7] Because of this, DB[*a,l*]P's presence in cigarette smoke and other sources of environmental exposure had not been quantified. Recent tests have shown DB[*a,l*]P to be one of the most potent of the carcinogenic PAHs, with greater tumor-inducing properties than DMBA – a synthetic compound formerly thought to be the most potent PAH [8,9].

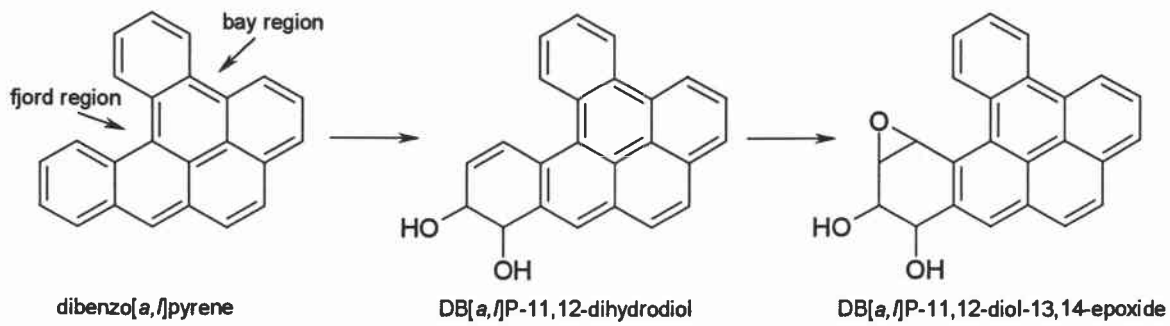

Figure 2: General pathway of metabolic activation of DB[*a,l*]P in the human mammary carcinoma cell line MCF-7. (12)

The metabolism of DB[*a,l*]P is complicated by the presence of an additional angular benzylic group which contributes to formation of a bay-region, as well as an area referred to as the "fjord-region". In theory this could lead to the formation of three different reactive diol-epoxide metabolites – the bay region metabolite DB[*a,l*]P-1,2-diol-3,4-epoxide, and the fjord-region metabolites DB[*a,l*]P-3,4-diol-1,2-epoxide and DB[*a,l*]P-11,12-diol-13,14-epoxide. [10] Studies have shown that only one of these is

actually formed, the DB[*a,l*]P-11,12-diol-13,14-epoxide (DB[*a,l*]PDE), which forms from the intermediate DB[*a,l*]P-11,12-dihydrodiol.[11,12,13] This diol-epoxide forms both *syn-* and *anti-* adducts with DNA.[12] These adducts interfere with DNA replication and can cause genetic mutations in humans and other vertebrates. Depending on the location of these mutations, deregulation or dysregulation of cellular growth can occur, leading to tumor formation.

Epidemiological studies in humans have linked a reduced risk for some types of tumors with consumption of certain foods, notably fruits and green or yellow vegetables.[14-16] A number of phytochemicals (chemical constituents of plants) have been identified that show chemopreventive activity in experimental carcinogenesis. These compounds can act by blocking initial DNA damage, or by interfering with post-initiation processes.

While many chemopreventive compounds are present in edible plants commonly consumed by humans, the concentrations ingested are likely to be considerably lower than the doses expected to show chemopreventive effects. An exception to this is the plant pigment chlorophyll, which is abundant in green and leafy vegetables, and could be realistically expected to be present in large enough quantities in the diet to have chemopreventive effects.

Chlorophyllin (CHL), the water-soluble derivative of chlorophyll, has been used for many years in the palliation or treatment of several medical problems. It has been used to accelerate wound healing[17,18] and to control body, urinary, and fecal odors in geriatric patients.[19] No toxicity, skin sensitization or other serious side effects have been

seen from the use of CHL in these cases.[17] The non-toxicity of CHL, combined with the abundance of its parent compound in the diet and its inhibitory activity in experimental carcinogenesis have led to considerable interest in CHL as a dietary chemopreventive agent.

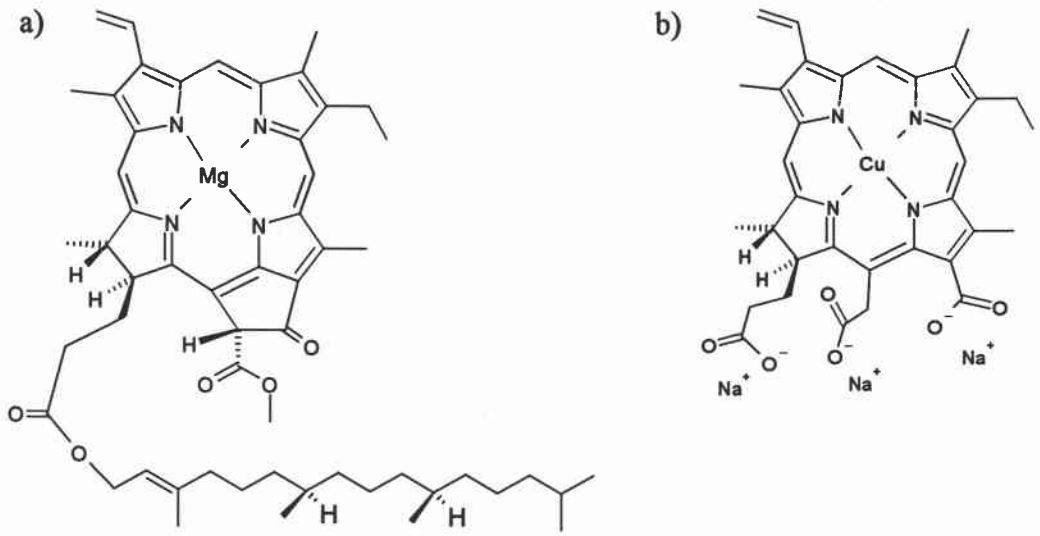

Figure 3: Structures of: a) chlorophyll a and b) sodium copper chlorophyllin

CHL has been shown to prevent DNA adduction by both aflatoxin B_1 (AFB_1) [20] and 2-amino-3-methylimidazo[4,5-f]quinoline (IQ) [21] when administered with the carcinogen. In a number of studies, it has been shown to reduce tumor incidence and/or multiplicity when given orally, including in dietary exposure of trout to AFB_1,[22] topical exposure of mice to BaP,[23] dietary exposure of rats to 2-amino-1-methyl-6-phenylimidazo[4,5-b]pyridine (PhIP),[24] and gavage of rats with IQ.[25] CHL in the diet has also been shown to reduce incidence of liver, stomach and swim bladder tumors from dietary exposure to DBP in rainbow trout.[26]

The mechanisms of CHL inhibition of carcinogenesis have been investigated with a number of compounds. Amongst these are IQ,[27] BaP,[28] and AFB_1.[29] These studies focused primarily on two mechanisms of inhibition: molecular complex formation and inhibition of carcinogen activation. Additionally, the BaP study examined the effects of CHL on time-dependent hydrolysis of the ultimate carcinogen (a diol-epoxide).

My study examines the mechanisms by which CHL inhibits DB[*a,l*]P carcinogenesis. Mechanisms by which CHL could prevent uptake and activation of DB[*a,l*]P were given the most consideration, with characterization of complex formation and investigation of inhibition of activation. Antimutagenesis assays utilizing the Ames test have examined the cumulative effect of CHL on DB[*a,l*]P mutagenesis. In addition to the other mechanisms studied, this antimutagenesic effect could be due to post-activation inhibition, such as complexation with or increase in hydrolytic rate of the ultimate carcinogen.

Materials and Methods

Chemicals. Dibenzo[*a,l*]pyrene was obtained from Chemsyn Science (Lenexa, KS). For fluorescence experiments DB[*a,l*]P was dissolved in spectrophotometric grade, inhibitor-free tetrahydrofuran (THF) (Aldrich, Milwaukee, WI). To prevent excessive peroxidation of THF during storage, solutions were stored under argon. Concentrations of DB[*a,l*]P in THF solution were verified spectrophotometrically, based on absorbance at 317 nm ($\varepsilon_{317} = 5.14 \times 10^{-4}$). For HPLC and mutagenicity assays, DB[*a,l*]P was dissolved in dimethylsulfoxide (DMSO). All solutions were stored at -4 ° C when not in use.

Note: DB[a,l]P is a potent carcinogenic compound. It was handled, stored and disposed of in compliance with Oregon State University guidelines for class C carcinogens.

Chlorophyllin (CHL) was obtained from Sigma (St. Louis, MO). Since commercially available CHL is a mixture of sodium copper chlorophyllin and several inorganic salts, all CHL solution concentrations were corrected for actual copper chlorophyllin content (51.3%). CHL has the property of self-association, resulting in a time-dependent reduction in effective concentration. Thus, for each experiment CHL was dissolved in the appropriate buffer immediately prior to use.

Since both CHL and DB[*a,l*]P are light sensitive compounds, all solutions containing either compound were protected from exposure to light. Experiments were done under subdued lighting whenever possible.

Salmonella typhimurium tester strain TA100 was kindly supplied by the B. N. Ames laboratory (UC Berkeley). All media used in the *Salmonella* mutagenicity assays was prepared as detailed by Maron and Ames.[30]

Instrumentation. Fluorescence experiments were carried out on an SLM 800C photon counting spectrofluorometer equipped with a 450 W xenon arc excitation source. Sample temperature was maintained by circulating water from a constant temperature bath through the cuvette holder. High performance liquid chromatography (HPLC) experiments utilized a Waters 2690 separations module with a Waters 996 photodiode array detector (PDA).

Complexation experiments:

Determination of optimum buffer composition for fluorescence quenching. Optimum buffer composition permitting maximum observable quenching was determined by titrating a constant amount of DB[*a,l*]P with CHL in a variety of buffer compositions. These compositions, expressed as % THF in 0.1 M tris at pH 7.4, were: 50, 30, 20, and 15. In each case, five 2 µl aliquots of DB[*a,l*]P solution were delivered by positive displacement pipet into 3 ml of buffer for a final DB[*a,l*]P concentration of 1.48 µM. Fluorescence (excitation 317 ± 8 nm, emission 425 ± 8 nm) was measured after each added DB[*a,l*]P aliquot to verify a linear fluorescence response. Each solution was then titrated with successive 2 µl aliquots of CHL solution, resulting in 0.2 µM concentration increases per aliquot up to a final CHL concentration of 4.4 µM. Fluorescence was measured after each addition.

Quenching of DB[*a,l*]P emission by CHL. To establish the quenching effect of CHL on the DB[*a,l*]P fluorescence spectrum, emissions from a 1.48 μM solution of DB[*a,l*]P in 20% THF in 0.1 M tris at pH 7.4 were measured from 400 to 500 (± 8) nm at an excitation of 317 ± 8 nm. Spectra were then replotted after each 1 μM incremental increase in CHL concentration, up to a final concentration of 5 μM.

In 20 % THF in 0.1 M tris at pH 7.4, DB[*a,l*]P fluorescence response began to lose linearity at concentrations above 1.2 μM. Thus experiments to quantify DB[*a,l*]P-CHL complex formation used a DB[*a,l*]P concentration of 1.18 μM, which maximizes the fluorescence within the linear range. Under excitation at 317 ± 8 nm, the fluorescence at 425 ± 8 nm at 25° C was measured with CHL concentrations ranging from 0.0 to 5.0 μM in 0.2 μM increments. At least two determinations were made at each of three replicates for each CHL concentration.

Preparation of CYP1A-induced trout liver microsomes.

Induction of CYP1A in trout. Rainbow trout (*Oncorhynchus mykiss*) were exposed to dietary β-naphthoflavone (BNF). BNF was dissolved by sonication in menhaden oil, which was then incorporated into Oregon Test Diet (OTD) for a dry diet composition of 500 ppm BNF. Trout weighing approximately 25 g were fed this diet for three days, with one feeding of approximately 0.02 g diet per g trout per day. On the third day trout were sacrificed by cervical spinal transection, their livers removed, and weighed, then placed in plastic vials, frozen in liquid nitrogen and stored at -80° C until use.

Abbreviations: DTE – dithioerythritol; EDTA – ethylenediaminetetraacetic acid; NADPH - β-nicotinamide adenine dinucleotide phosphate, reduced form; PMSF – phenylmethylsulfonyl fluoride

Preparation of microsomes. Pooled livers were homogenized in four volumes of homogenization buffer (100 mM tris, 100 mM KCl, 1mM EDTA, 0.5 mM PMSF, 1 mM DTE) using an Potter-Elvejhem apparatus with a motor driven pestle. The homogenate was centrifuged for 20 min at 10,000 x g in a pre-cooled (4° C) Beckman type 70 rotor. Supernatant was removed and further centrifuged for 90 min at 100,000 x g. The resulting supernatant was discarded, and the pellet was resuspended in one volume resuspension buffer (100 mM pH 7.3 potassium phosphate, 1 mM EDTA, 20% glycerol, 1 mM DTE). Microsomal preparations were stored at -80° C.

Analysis of microsomal preparation. Microsomal protein content was determined by the Lowry method.[31] Briefly, 10 µl of diluted microsomal preparation was mixed with 1 ml of 2 % Na_2CO_3 / 0.02 % sodium potassium tartrate / 0.01 % $CuSO_4$ and allowed to incubate for 10 min, after which 100 µl 50 % Folin-Ciocalteu's Phenol reagent was added. After 30 min the spectrophotometric absorbance of the mixture was determined at 750 nm, and compared to a standard curve of bovine serum albumin solutions to estimate protein concentration. Induction of CYP1A enzymes was tested by measuring the rate of ethoxyresorufin O-deethylation (EROD) in the presence of microsomes and NADPH using the method of Burke.[32]

***Salmonella* mutagenicity test.**

Tester strain growth and storage. *Salmonella typhimurium,* strain TA 100 was grown overnight at 37° C in Oxoid nutrient broth #2. Before making the frozen permanents the genotype of TA100 was confirmed using the method of Maron and Ames.[30] Permanent stocks were made by dissolving 0.18 ml DMSO into 2 ml aliquots of

freshly grown TA100 culture in cryotubes. These mixtures were then rapidly frozen under liquid nitrogen for storage at -80° C. For master plates, cultures were streaked for isolation on histidine / biotin / ampicillin minimal glucose plates, grown for 24 hours at 37° C and stored at 4° C for up to one month. Isolated colonies from these master plates were used to inoculate cultures for use in the mutagenesis assays.

Mutagenesis assays. To increase the sensitivity of the assays, DB[*a,l*]P, CHL, and TA100 were pre-incubated with microsomes in the presence of NADPH before plating. Each experiment included platings of pre-incubation mixture without DB[*a,l*]P to monitor spontaneous reversion rates. Spot tests on a separate plate were used for controls, with 1.0 μg sodium azide per spot for the positive control and 5.0 μg daunomycin per spot for the negative. Assays were run at five CHL doses: 0, 0.1, 1, 10 and 50 nmol/plate, with at least three plates at each dose. Pre-incubations containing STKM buffer (250 mM sucrose, 80 mM tris, 25 mM KCl, 5 mM MgCl; pH 7.4), 250 μg microsomal protein, 3 mM NADPH, the CHL doses in STKM, 100 μl of fresh TA100 culture were initiated by the addition of 10 nmol DB[*a,l*]P in 10 μl DMSO. Total pre-incubation volumes were 250 μl. After a 30 minute incubation at 25° C the pre-incubation mixture was transferred to a tube containing 2 ml of top agar (6 % agar, 5% NaCl) and 0.25 ml 0.5 mM histidine / biotin solution held at 45°C. Each tube was vortexed gently then poured onto minimal glucose medium plates. Following solidification of top agar the plates were inverted and incubated at 37° C in the dark for 48 hours. Wild-type (his^+) revertants were counted manually.

Analysis of metabolism by high performance liquid chromatograpy (HPLC) separation.

Incubation with CYP1A-induced microsomes. DB[*a,l*]P was incubated with microsomes, NADPH and varied concentrations of CHL to examine the possibility of CHL inhibition of DB[*a,l*]P metabolism. Final reaction volumes totaled 125 µl consisting of STKM, 1 mg/ml microsomal protein, 3 mM NADPH, varied concentrations of CHL in STKM. The reactions were initiated by addition of 62.5 µM DB[*a,l*]P in 10 µl DMSO (5 µM total DB[*a,l*]P concentration). Tubes were vortexed and incubated at 13° C (typical trout environmental temperature) for 20 minutes.

At the end of the incubation period, 5 µl of 80 µM benzo[*a*]pyrene was added to each sample as an internal standard. To terminate the *in vitro* metabolic reactions and precipitate the proteins, 250 µl acetone and 250 µl acetone : methanol 1:1 were added to the samples, which were then stored at -20° C for at least two hours. After centrifugation at 15,000 x g for 5 minutes to pelletize the precipitated proteins, 0.5 ml of supernatant was removed and placed in an amber sampling vial containing 675 µl of 1:1 acetone:methanol.

Analysis of samples on reversed-phase HPLC. Sample compartment temperature in the HPLC was held at 10° C to maintain the stability of the metabolites. Samples of 100 µl were injected onto a 150 x 4.6 mm C-18 Spherisorb ODS-2 column protected by a 30 mm guard column. Column temperature was maintained at 35°C by a column heater. Sample components were eluted with a methanol/water gradient over a period of 35 minutes at 1 ml per minute. To allow re-equilibration of the column, each injection was delayed ten minutes from the end of the last gradient. Baseline control

gradients were begun with an injection of methanol alone. Methanol was injected after every fifth sample to monitor the baseline and observe for aberrant peaks.

Peaks were tentatively identified based on retention time and verified by comparison of the photodiode array detector (PDA) spectra with those of known standards. The area for each metabolite peak was divided by the area of the internal standard peak to give a ratio that was used to compare the quantities of metabolites between samples.

Results and Discussion

Fluorescence quenching experiments.

Many optical methods exist for characterization of complex formation, including UV/visible spectrophotometry, refractometry, and fluorescence spectroscopy. Fluorescence spectroscopy has the advantage of high molar sensitivity,[33] which allows work with less soluble compounds such as DB[*a,l*]P that can not be put into aqueous solution in high concentrations. For measurement of complex formation with fluorescence methods, a change in the steady state fluorescence of one or both of the compounds must occur upon complexation. In the case of the CHL-DB[*a,l*]P complex, the measured change was a quenching of the DB[*a,l*]P fluorescence with complex formation.

The predominantly planar conjugated structure of both compounds allows for complex formation between CHL and DB[*a,l*]P. The complex is believed to be held together by numerous face-to-face π-π orbital overlaps. At the close intermolecular distances involved in such a complex, fluorescence quenching occurs through a radiationless energy transfer from the excited state of the fluorescent molecule (DB[*a,l*]P) to the ground state of the quenching molecule (CHL).[34] Fluorescence measurements taken during titration of a solution of DB[*a,l*]P with CHL give an indirect measurement of the amount of complexed DB[*a,l*]P. These data can be used to determine binding affinity (given as a dissociation constant (K_d)) and stoichiometry of the complex.

Preliminary experiments using a buffer composition of 50 % THF in 0.1 M Tris at pH 7.4 resulted in no fluorescence quenching attributable to complex formation; the

measured loss in fluorescence was due almost entirely to CHL absorbance at both emission and excitation wavelengths.

With a buffer composition of 15 % THF in 0.1 M Tris at pH 7.4, DB[*a,l*]P gave a pronounced non-linear response. For this reason, DB[*a,l*]P in 15 % THF was not titrated with CHL, and this buffer was not used further in quenching experiments. For all other buffer compositions tested, data were plotted for comparison. The fluorescence for a given data point (F_m) was subtracted from the fluorescence of DB[*a,l*]P alone (F_o) to give the change in fluorescence (ΔF):

$$\Delta F = F_o - F_m$$

Dividing ΔF by F_o gives the fraction of fluorescence quenched. Plots of $\Delta F / F_o$ versus CHL concentration (Figure 4) were used to compare quenching at the different buffer compositions.

An apparent increase in fluorescence quenching was seen with a decrease in THF composition. While a greater quenching effect was seen with 30 % THF than with 25 %, this could be due to experimental error, as determinations were only done once with each of these two buffers. The greatest degree of quenching was seen with 20 % THF, which was the lowest THF composition tested where DB[*a,l*]P still showed a linear fluorescence response. This lead to the use of 20 % THF in 0.1 M Tris at pH 7.4 for all further fluorescence experiments.

Titration of DB[*a,l*]P with CHL resulted in a uniform quenching of the fluorescence emissions between 400 and 500 (±8) nm, as shown in Figure 5. No peak shifts or changes in fluorescence characteristics other than quenching were observed in this experiment.

CHL has some absorbance at both the excitation and emission wavelengths at the maximum concentration used in the titrations (5 μM). This effect was deemed to be negligible after it was shown that there was no quenching effect on the light scattered by 20 % THF buffer containing the concentrations of CHL used in the experiments. These concentrations were considerably lower, i.e. 1/10, than the concentrations used in the preliminary experiments wherein almost all loss of fluorescence was attributable to CHL absorbance of light. CHL also has a lower molar absorptivity in the 20% THF buffer than in the 50%, which further reduces interference by absorbance effects.

Data from CHL titrations of DB[*a,l*]P solution were analyzed using an iterative modeling process. Data were first modeled assuming a 1:1 CHL to DB[*a,l*]P stoichiometry. The model for a 1:1 ratio of CHL to DB[*a,l*]P binding was constructed as follows:

$$\text{CHL} + \text{DB}[a,l]\text{P} \underset{}{\overset{K_d}{\rightleftharpoons}} \text{CHL-DB}[a,l]\text{P}$$

The dissociation constant (K_d) for this system is given as:

$$K_d = \frac{[\text{CHL}]\ [\text{DB}[a,l]\text{P}]}{[\text{CHL-DB}[a,l]\text{P}]}$$

Fraction of fluorescence quenched for each data point was calculated as in the buffer composition experiments. Plots of $\Delta F / F_o$ vs. CHL concentration were used to fit data sets to the model. Fit of the data to the 1:1 model is shown in Figure 6.

The residuals give a measure of how well the data fit the model. They are calculated as the successive differences between $\Delta F / F_0$ data points and the fitted curve (F_f). A non-random trend is apparent in the residuals for the 1:1 model (Figure 7a),

which is indicative of a poor fit to the model. Because of this poor fit, a 2:1 CHL to DB[*a,l*]P model was considered. The model for a 2:1 ratio of CHL to DB[*a,l*]P binding was constructed as follows:

$$2\ \text{CHL} + \text{DB}[a,l]\text{P} \overset{K_{d1}}{\rightleftharpoons} \text{CHL} + \text{CHL-DB}[a,l]\text{P} \overset{K_{d2}}{\rightleftharpoons} \text{CHL}_2\text{-DB}[a,l]\text{P}$$

The dissociation constants (K_{d1} and K_{d2}) for this system are given as:

$$K_{d1} = \frac{[\text{CHL}]\ [\text{DB}[a,l]\text{P}]}{[\text{CHL-DB}[a,l]\text{P}]} \qquad K_{d2} = \frac{[\text{CHL}]\ [\text{CHL-DB}[a,l]\text{P}]}{[\text{CHL}_2\text{-DB}[a,l]\text{P}]}$$

While the 1:1 model assumed complete quenching of fluorescence for a DB[*a,l*]P molecule upon complexation with CHL, the 2:1 model allows for differences between the two complexes. The total fluorescence (F_{tot}) of the system is given by:

$$F_{tot} = F\ [\text{DB}[a,l]\text{P}] + p_1 F\ [\text{CHL- DB}[a,l]\text{P}] + p_2 F\ [\text{CHL}_2\text{ - DB}[a,l]\text{P}]$$

Where p_1 and p_2 are the fluorescence enhancements for the complexes CHL- DB[*a,l*]P and CHL_2 - DB[*a,l*]P respectively, and F is the molar fluorescence of DB[*a,l*]P. Fit of data sets to the 2:1 model is shown in Figure 8. Residuals for this model (figure 7b) showed no apparent trend, which suggests a good fit of the data to the curve.

The number of variable unknowns in the 2:1 model (K_{d1}, K_{d2}, p_1 and p_2) makes it necessary to make some assumptions about the system in order to arrive at a value for the dissociation constants. The simplest model assumes that the two dissociation constants are equal ($K_{d1} = K_{d2}$) and that the fluorescence enhancement for each complex is equal to zero ($p_1 = p_2 = 0$). For this model, the curves showed a very good fit ($R^2 = 0.9997$) and

gave a value of K_d = 1.59 μM (σ = 0.01). The system was also modeled allowing differential K_ds and different fluorescence enhancements for the two complexes. One such model, where p_1 = 0.185, gave a very good fit (R^2 = 0.9998) and inferred dissociation constants of: K_{d1} = 1.29 μM (σ = 0.03) and K_{d2} = 1.01 μM (σ = 0.04). Other parameter variations under this second scheme also provided satisfactory fits, yielding dissociation constants ranging between 1.0 and 1.9 μM.

The smaller a dissociation constant is, the stronger the binding of the complex. The range of dissociation constants inferred for CHL-DB[*a,l*]P in this study is very similar to the published value for CHL-aflatoxin B_1 complexation (1.4 ± 0.4 μM)[29]. It represents considerably stronger binding than the dissociation constants calculated for complexation between CHL and several heterocyclic amines, which ranged from 78.5 μM for 3-amino-1,4-dimethyl-5*H*-pyrido[4,3*b*]-indole (Trp-P-1) to 326 μM for 2-amino-6-methyldipyridol[1,2-*a*:3',2'-*d*]imidazole (Glu-P-1).[35]*

The binding of two CHL molecules to a single molecule of DB[*a,l*]P would result in an aggregate molecular weight greater than five times that of the uncomplexed PAH. Such a large complex may be expected to reduce uptake of DB[*a,l*]P from the digestive tract, as larger molecules are generally not as easily absorbed.

CYP1A-induced microsomal preparations.

Cellular homogenization results in fragmentation of endoplasmic reticulum (ER). Under appropriate conditions these ER fragments spontaneously close to form vesicles called microsomes. Microsomes can be separated from other cellular components via

* Results in this study were given as binding constants (Kbs). For consistency, they were converted to dissociation constants using the equation: $K_d = 1/K_b$.

differential centrifugation.[36] Among the enzymes contained in these microsomes are cytochrome P-450s, which are responsible for PAH activation. Since some cytochrome P-450s are inducible enzymes, the levels contained within the microsomes can be increased by pre-treatment of the source tissue with an inducer. In these experiments, rainbow trout were fed diet containing β-naphthoflavone, a well-characterized CYP1A inducer. Livers of these trout were used to make CYP1A-induced microsomes. These induced microsomes provide a biologically relevant means to activate PAHs in *in vitro* experiments.

Preparation of microsomes involves separation of the microsomes from the cytosolic fraction. The absence of certain enzymes found in the cytosolic fraction needs to be taken into account when microsomes are used as in *in vitro* experiments. Most notably absent in these experiments is the primarily cytosolic enzyme epoxide hydrolase. This catalyzes the ring opening of the initially formed epoxide, forming the DB[*a,l*]P-11,12-dihydrodiol (DB[*a,l*]P-DHD) intermediate. Thus for both Salmonella mutagenicity tests and metabolism experiments epoxide hydrolase should have been added to increase the rate of DB[*a,l*]P-DHD formation.

Research into the CYP1A sub-family has identified at least two different trout 1A genes.[37] Evidence indicates that these genes are differentially regulated.[38] This means that the two gene products may be produced in different proportions with BNF induction than they would be with DB[*a,l*]P induction. In view of this, it would be advisable to include microsomes induced with DB[*a,l*]P in future work.

Antimutagenicity in the *Salmonella* mutagenicity assay.

Detection of mutagenesis by the *Salmonella* mutagenicity test relies on the tester strain carrying a mutation in the histidine biosynthetic operon that renders the strain histidine dependent (his^-).[30] If a compound can cause a mutation at this same site that reverts the organism to wild type, the organism regains the ability to synthesize histidine (his^+) and therefore grows on histidine deficient media. The number of revertant colonies formed after exposure to several different doses of a compound can be used to quantify mutagenic potency. Similarly, addition of different doses of an inhibitor to a constant dose of mutagen is useful in evaluating the antimutagenic potential of the inhibitor against that mutagen.

Tester strains have been developed to test for different types of mutagens, specifically, point mutagens (strains TA100 and TA1535), frameshift mutagens (TA98 and TA1538) and cross-linking agents (TA102). Based on recent studies of DB[*a,l*]P activation and adduction,[10] it was expected to act as a point mutagen in this assay. Strain TA100 was chosen over TA1538 for increased sensitivity; it carries a plasmid that enhances error-prone repair in the cell.

Spontaneous reversion rates were within the range reported as characteristic for TA100.[30] A nearly 30 % reduction in revertant colonies was seen when spontaneous reversion controls (no added mutagen) were assayed without addition of microsomes. This phenomenon indicates that even in the absence of added mutagen, the microsomal preparation itself may have some mutagenic properties.

A significant decrease in mutagenicity was seen with the addition of very small quantities of CHL relative to DB[*a,l*]P in this assay. (Figure 9) Based on mean values, more than 50% inhibition of mutagenesis was seen at a CHL concentration only one tenth that of DB[*a,l*]P, and slight inhibition was seen even when DB[*a,l*]P exceeded CHL by 100-fold. Inhibition at such low molar ratios of CHL to DB[*a,l*]P suggests that complex formation between the two compounds is not the major mechanism responsible for antimutagenesis in these experiments. One possibility is that CHL is interfering directly with the CYP1A enzymes. This would make inhibition a function of the ratio of CHL to enzyme rather than CHL to DB[*a,l*]P. This hypothesis seems reasonable, as CHL has been demonstrated to have a concentration-dependent inhibition of ethoxyresorufin O-deethylation,[28] a reaction mediated by CYP1A enzymes. An interesting observation that may support this theory is that revertant colony counts on plates with a CHL dose of 50 nmol were consistently lower than spontaneous reversion rates (with microsomes). While this would normally be an indication of toxicity, this CHL dose is in the non-toxic range determined by earlier antimutagenesis studies.[39,40] Direct interaction of CHL with the enzymes could not only be preventing activation of DB[*a,l*]P, but also may be interfering with the slight mutagenic properties of the microsomes that were mentioned earlier.

DB[*a,l*]P acts as a weak mutagen on TA100 in these assays. In a previous study,[11] the maximum number of revertants obtained was only about twice the spontaneous reversion rate. Our changes to the pre-incubation procedure increased this to about three times the spontaneous reversion rates. It should be noted that plate counts were still considerably lower than those obtained with other mutagens, including B[*a*]P.

Epoxide hydrolase was not added to these assays, which could reduce intermediate DB[*a,l*]P-DHD formation and therefore reduce production of the ultimate carcinogen. This does not seem to account for the low activity of DB[*a,l*]P however, as the earlier DB[*a,l*]P mutagenicity study [11] used liver S9, a preparation that contains the cytosolic fraction, for activation.

A possible reason for the weak activity of DB[*a,l*]P in these assays may be the nucleoside identity of the point mutation in TA100. This mutation, *hisG46*, replaces a wild type -$^{GAG}_{CTC}$- (leucine) with -$^{GGG}_{CCC}$- (proline) in the gene coding for ATP phosphoribosyl transferase, the first enzyme in histidine biosynthesis. [41] To cause a reversion to wild type, DB[*a,l*]P would need to form a deoxyguanosine or deoxycytidine adduct. While it does form deoxyguanosine adducts to some extent, studies have shown that the predominant DB[*a,l*]PDE adduct formed is with deoxyadenosine residues. [42,43,44] This could explain why B[*a*]P, which when activated binds predominantly to deoxyguanosine [45,46] is more mutagenic with TA100,[11] even though it is a weaker carcinogen than DB[*a,l*]P.[8,9] Recently developed *Salmonella* tester strains are available commercially (Xenometrix, Boulder, CO) that test for base-specific point mutations. [47] The use of one of these strains which has deoxyadenosine as a target residue (TA7001-TA7003) may be more appropriate for evaluation of mutagenesis and antimutagenesis involving DB[*a,l*]P.

Metabolites from HPLC analysis.

Several different DB[*a,l*]P metabolites could possibly result from the incubation of DB[*a,l*]P with CYP1A-induced microsomes. If CHL interferes with this metabolism, either through interaction with the enzyme or the DB[*a,l*]P itself, a reduction in the

quantity of metabolites would be expected. In order to examine this reduction in metabolite formation, it is necessary to separate and quantify the metabolites resulting from incubations run either with or without added CHL.

An effective method for such a separation is reversed phase high performance liquid chromatography (HPLC). Reversed phase HPLC utilizes a polar mobile phase and a non-polar stationary phase to separate samples into their constituent components. While a number of factors affect this separation, similar molecules will elute in the order of increasing hydrophobicity. Since metabolites of DB[*a,l*]P are essentially substituted forms of the base DB[*a,l*]P molecule, it is possible to predict the approximate order of elution for DB[*a,l*]P metabolites. The more highly hydroxylated metabolites, such as DB[*a,l*]P-11,12-dihydrodiol, would be expected to elute earlier in the separation. The identity and quantity of each peak in the resulting chromatogram can often be determined based on PDA spectral information. The effect of added CHL on DB[*a,l*]P metabolism was investigated in this way.

Four major PAH peaks were identified in the incubations of DB[*a,l*]P in the absence of CHL. These peaks, with their approximate retention times, were identified as: DB[*a,l*]P-11,12-dihydrodiol – 19.5 min., 7-hydroxy- DB[*a,l*]P – 22.4 min, B[*a*]P (internal standard) – 24.3 minutes, and DB[*a,l*]P – 26.6 min. Other peaks were also present in these separations, but control experiments and examination of PDA spectra led to the conclusion that these resulted from non-PAH components of the incubations. The major metabolite seen in these separations was the 7-hydroxy- DB[*a,l*]P form, however these incubations were done without addition of epoxide hydrolase. The low levels of

DB[*a,l*]P-11,12-dihydrodiol formed in these incubations is consistent with the absence of this enzyme.

Chromatogram I in Figure 10 is representative of DB[*a,l*]P metabolism in the absence of CHL. Peaks identified are A: DB[*a,l*]P-11,12-dihydrodiol; B: 7-hydroxy-DB[*a,l*]P; C: B[*a*]P; and D: DB[*a,l*]P. Chromatograms II and III represent 50 μM and 100 μM added CHL respectively. The two arrows above these chromatograms indicate the emergence of a peak which interferes with the 7-hydroxy-DB[*a,l*]P peak. Examination of the PDA spectrum of this peak shows a spectrum consistent with CHL or one of its derivatives. This peak began to emerge at CHL concentrations as low as 25 μM. At higher CHL concentrations several peaks with similar spectra appeared, including peaks at 19 and 20 minutes that interfere with the DB[*a,l*]P-DHD peak. The presence of these interfering peaks confounds interpretation of results at most CHL concentrations tested. In order to effectively look at the inhibition of DB[*a,l*]P metabolism by CHL the separation method (i.e. the column or the gradient) would need to be changed.

Conclusions

Based on fluorescence quenching data, a fairly strong (K_d = 1.0 – 1.9 μM) complex is formed between CHL and DB[*a,l*]P, with a 2:1 CHL : DB[*a,l*]P stoichiometry. Because of this strong complexation, dietary CHL could act to significantly reduce the uptake of DB[*a,l*]P from the gut, thereby reducing the overall exposure of animal.

In the Ames assay, CHL was antimutagenic at a fraction of the concentration of DB[*a,l*]P present. For this reason, complex formation is unlikely to account for any significant portion of the antimutagenesis in these experiments. The antimutagenic effect could be due to the CHL interfering directly with the CYP1A proteins, or to a CHL mediated increase in the rate of hydrolysis of the ulitmate carcinogen. Further experiments would be necessary to determine which of these mechanisms is responsible for the observed antimutagenic effect.

HPLC results were inconclusive, due to problems with the methods as explained in the results section. Modifications to these methods are necessary to observe the effects of CHL on the metabolism of DB[*a,l*]P by CYP1A-induced trout liver microsomes.

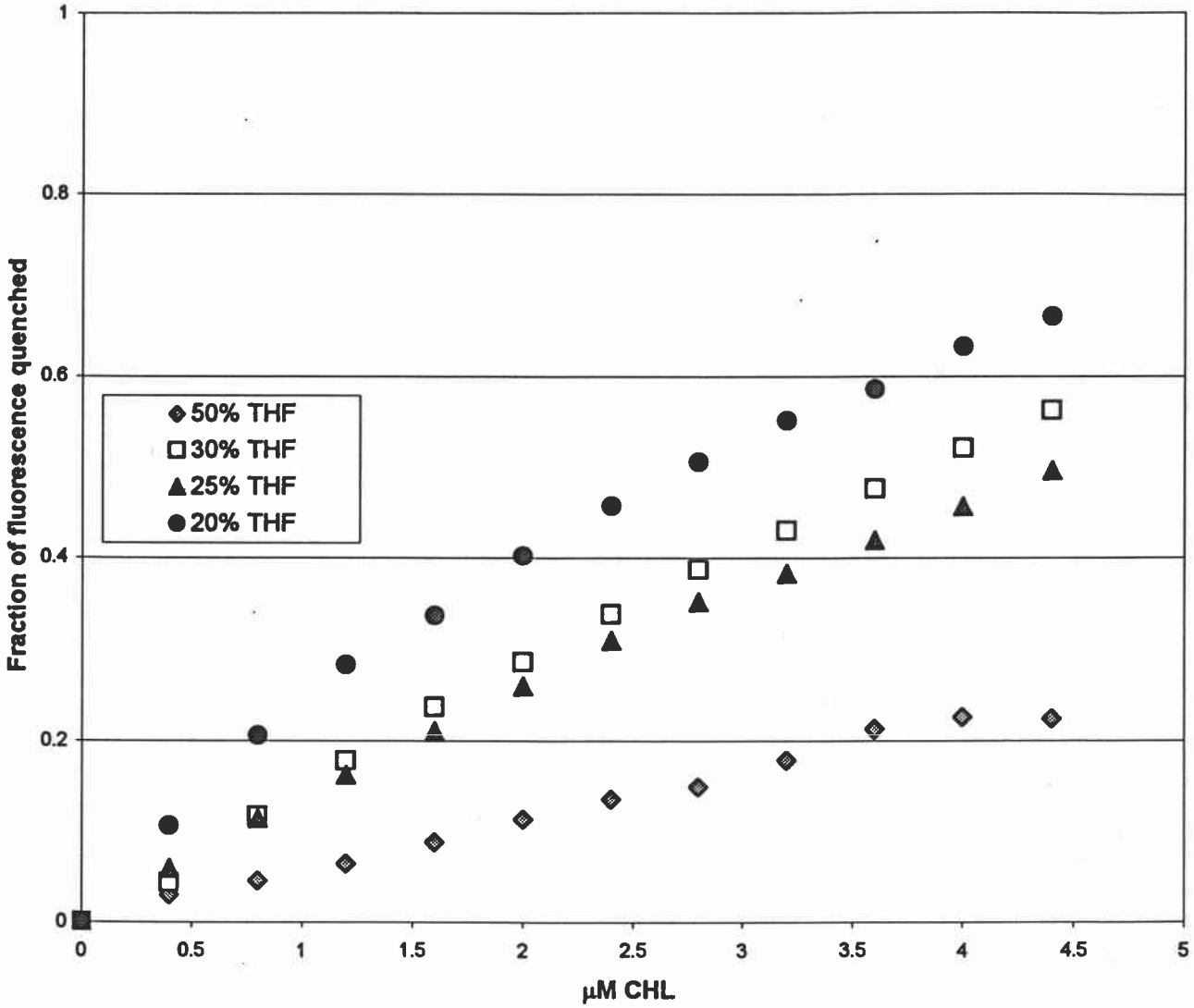

Figure 4: DB[*a,l*]P was titrated with CHL in buffers containing different concentrations of THF to determine the effect of buffer composition on observable quenching. Fluorescence determinations were made after each increment of CHL (ex: 317 ± 8 nm, em: 425 ± 8 nm); values obtained were normalized to fraction of fluorescence quenched for comparison. An increase in observable quenching was seen with a decrease in THF content; a buffer composition of 20% THF in 0.1 M Tris at pH 7.4 was selected for further complexation experiments.

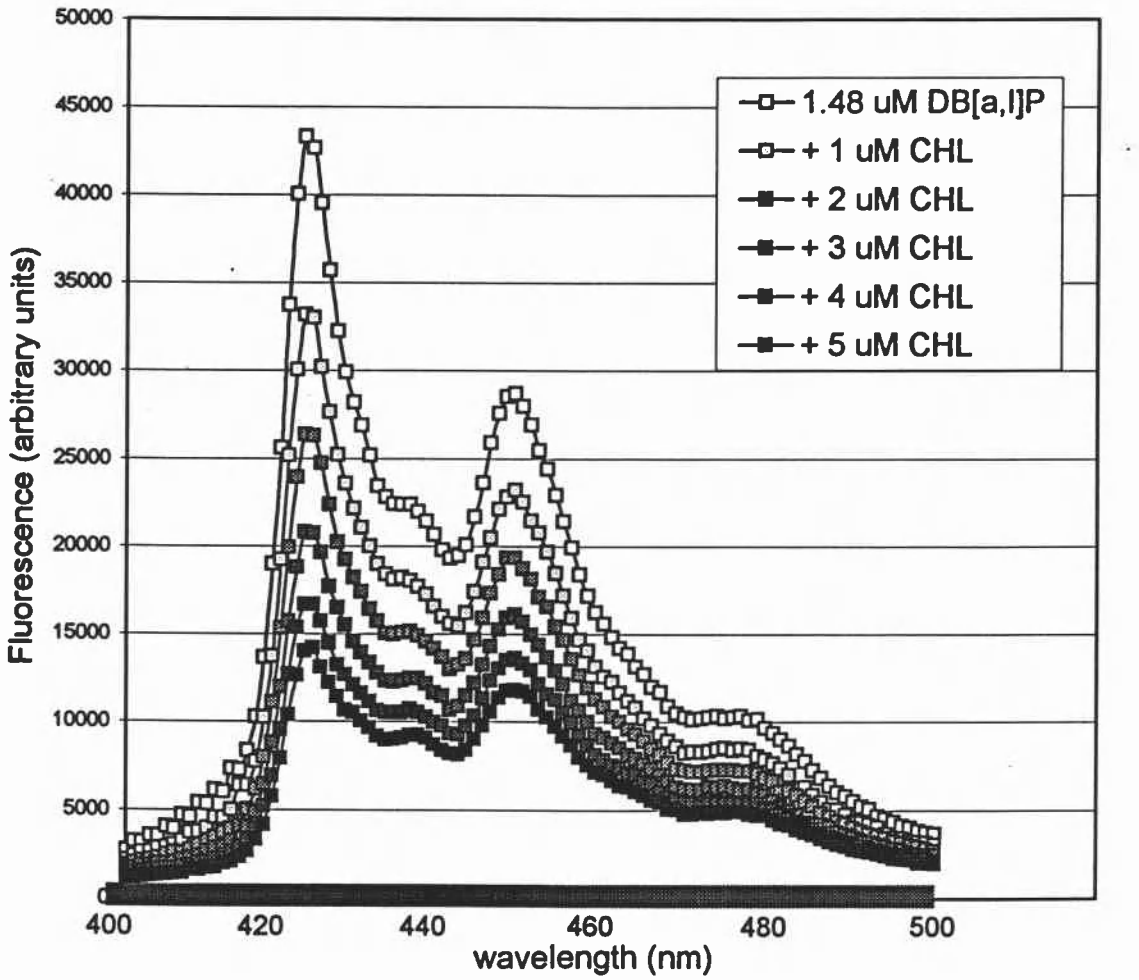

Figure 5: The emission spectrum from 400 to 500 (± 8) nm (ex: 317 ± 8 nm) was read for 1.48 μM DB[*a,l*]P alone, and following each 1 μM increment of CHL. The resulting spectra were plotted to observe the quenching effect of CHL on emission by DB[*a,l*]P.

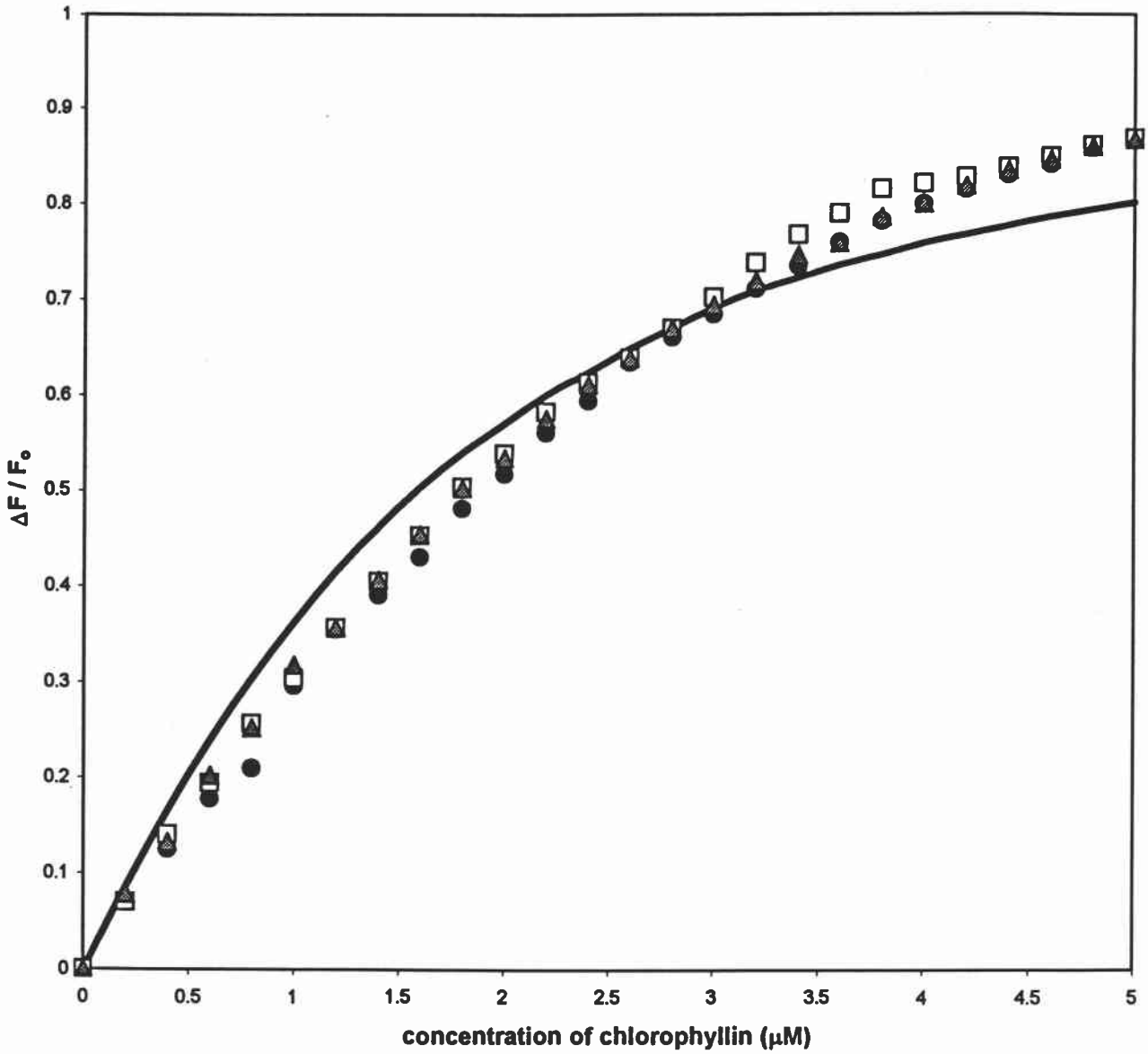

Figure 6: Fit of data to the 1:1 CHL: DB[*a,l*]P complexation model. DB[*a,l*]P (1.18 μM) was titrated with 0.2 μM increments of CHL to a final concentration of 5 μM CHL. The fluorescence was measured (ex: 317 ± 8 nm, em: 425 ± 8 nm) after initial addition of DB[*a,l*]P and following each increment of CHL. Data were normalized by converting fluorescence measurements to $\Delta F / F_o$ (page 15). Plots of $\Delta F / F_o$ vs. CHL concentration were used to fit the data to the 1:1 model. The three symbols represent three separate titrations, while the solid line represents the fitted curve.

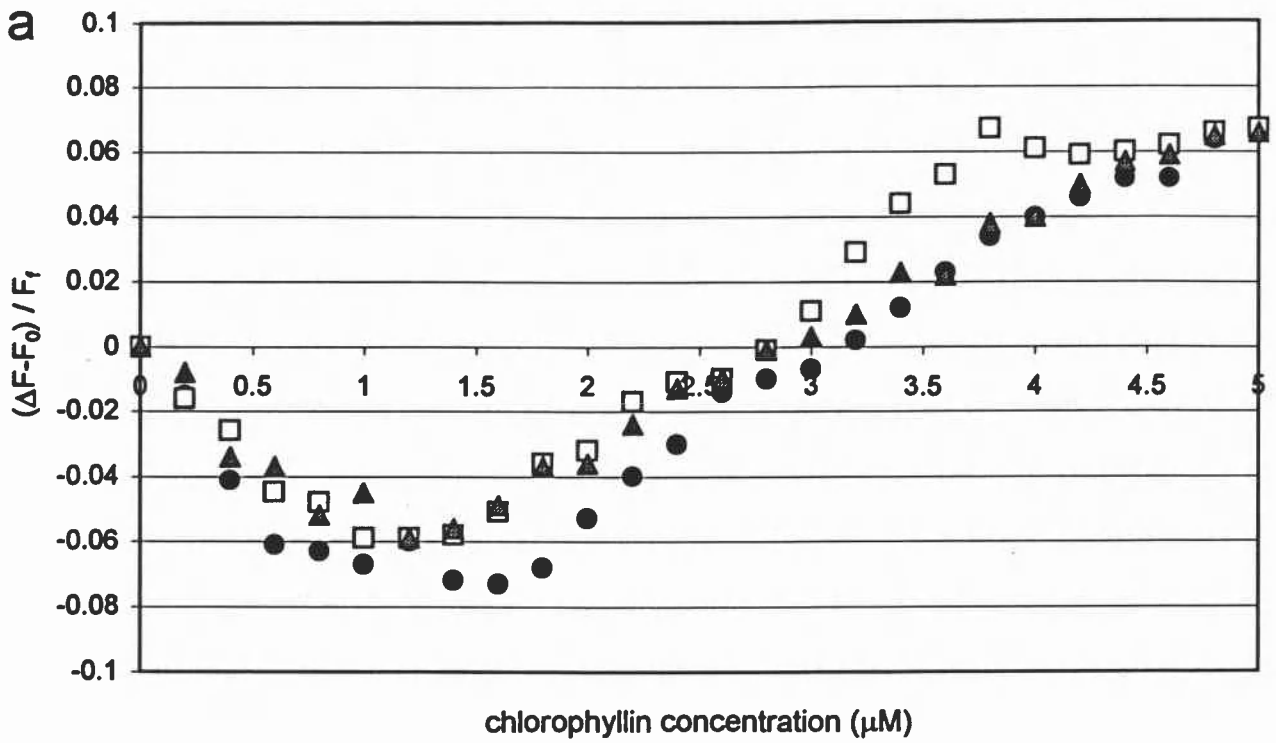

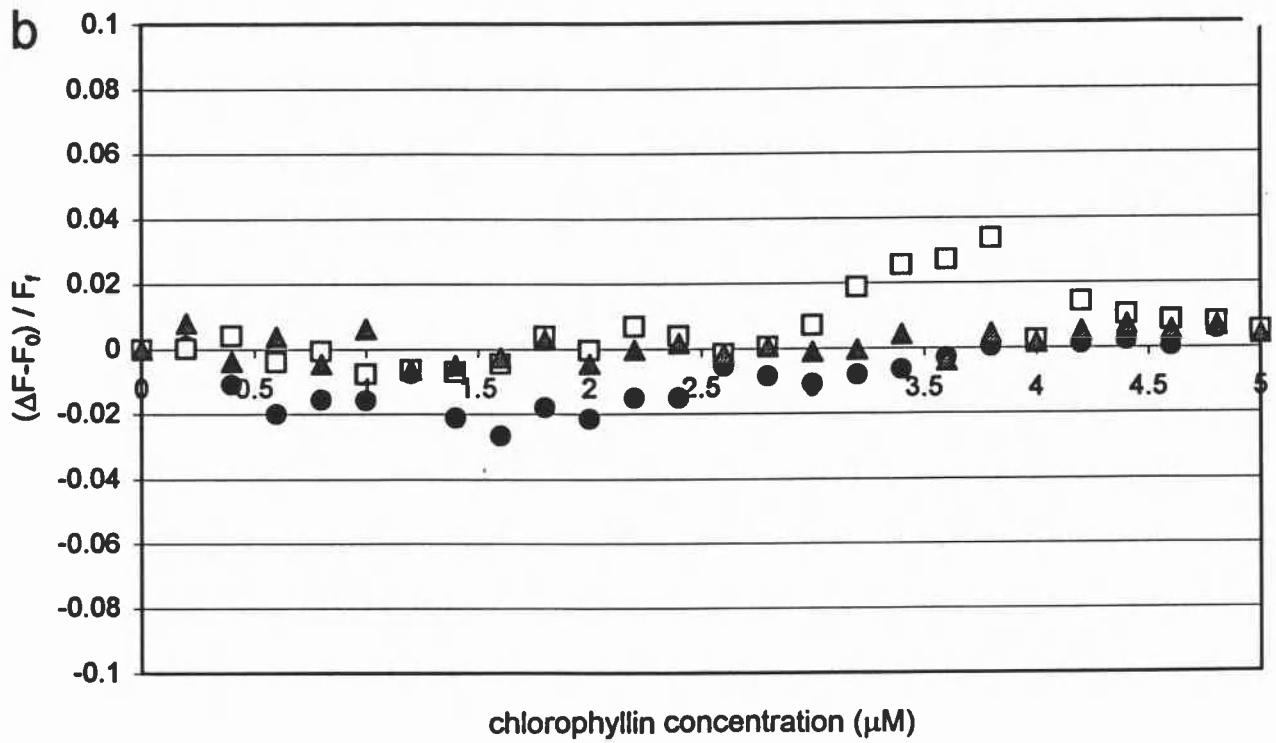

Figure 7: a) Residuals from 1:1 CHL: DB[*a,l*]P curve fit, as described on page 16. b) Residuals from 2:1 CHL: DB[*a,l*]P curve fit. The three symbols represent the three titrations.

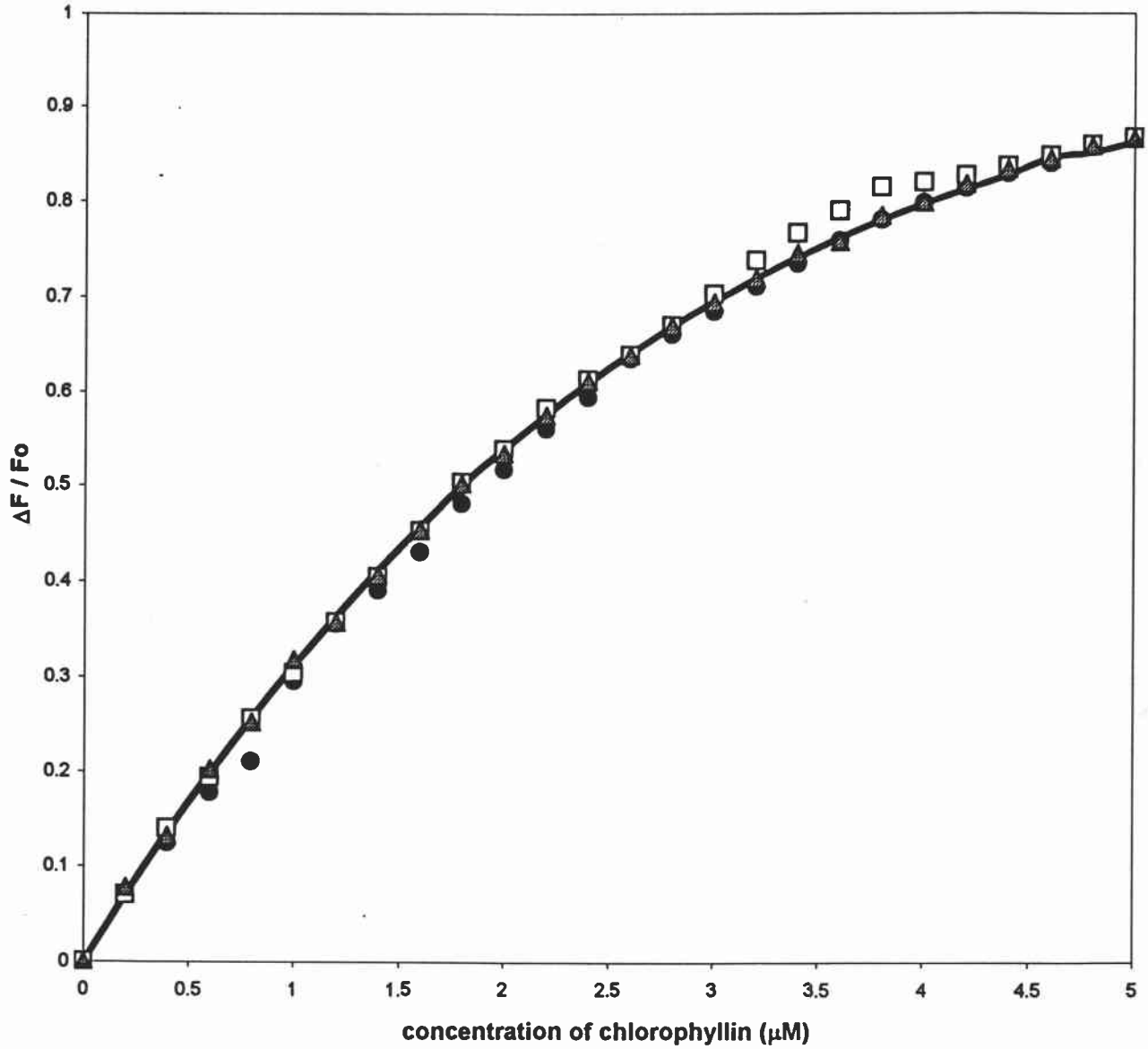

Figure 8: Fit of data to the 2:1 CHL: DB[*a,l*]P complexation model. DB[*a,l*]P (1.18 μM) was titrated with 0.2 μM increments of CHL to a final concentration of 5 μM CHL. The fluorescence was measured (ex: 317 ± 8 nm, em: 425 ± 8 nm) after initial addition of DB[*a,l*]P and following each increment of CHL. Data were normalized by converting fluorescence measurements to $\Delta F / F_o$ (page 15). Plots of $\Delta F / F_o$ vs. CHL concentration were used to fit the data to the 2:1 model. The three symbols represent three separate titrations, while the solid line represents the fitted curve.

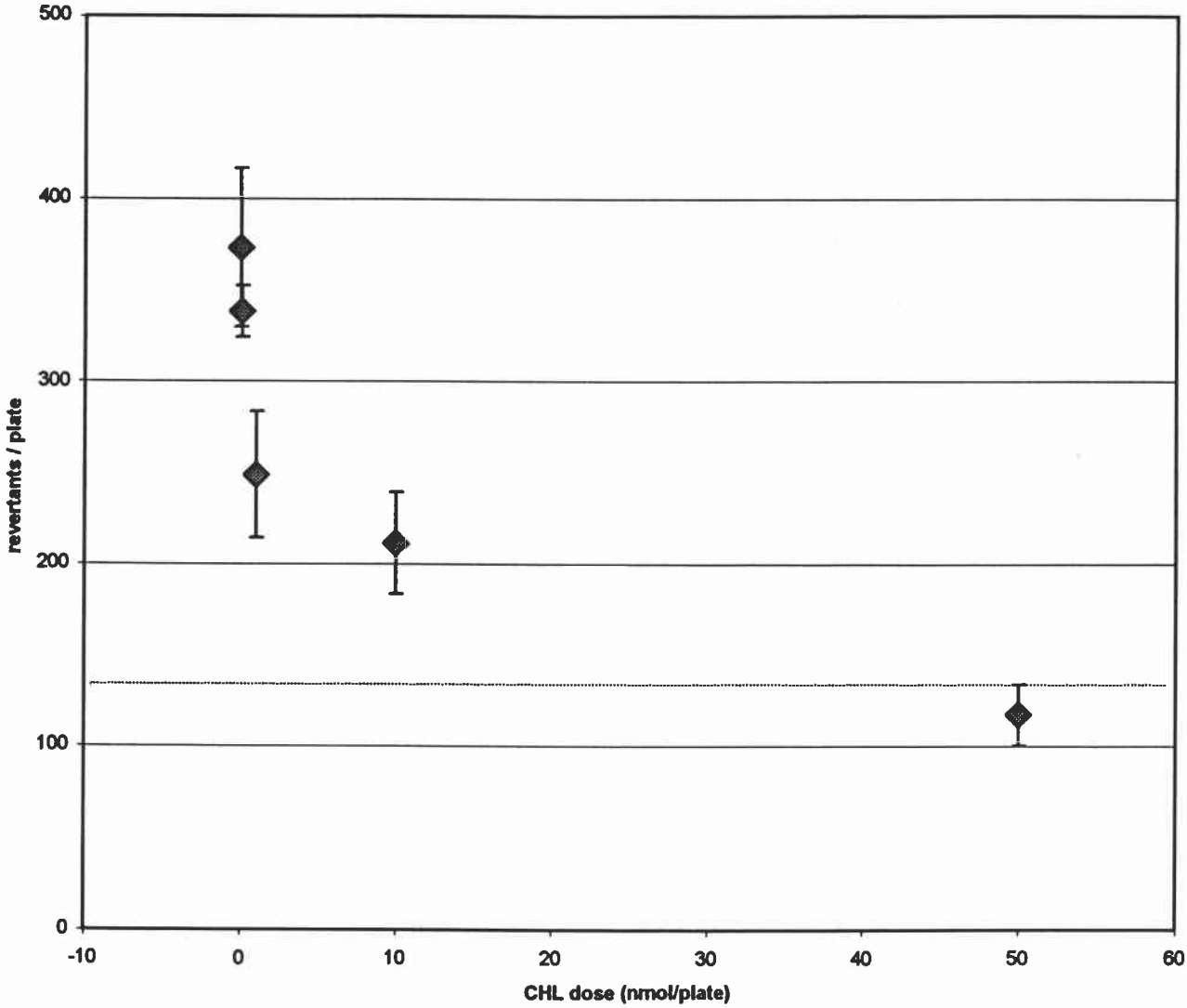

Figure 9: Inhibition of DB[a,*l*]P mutagenesis by CHL in the Ames test. Values for the y-axis are mean uncorrected plate counts (± SD). All plates had a constant dose of DB[a,*l*]P (10 nmol). The dotted line represents average spontaneous reversion counts.

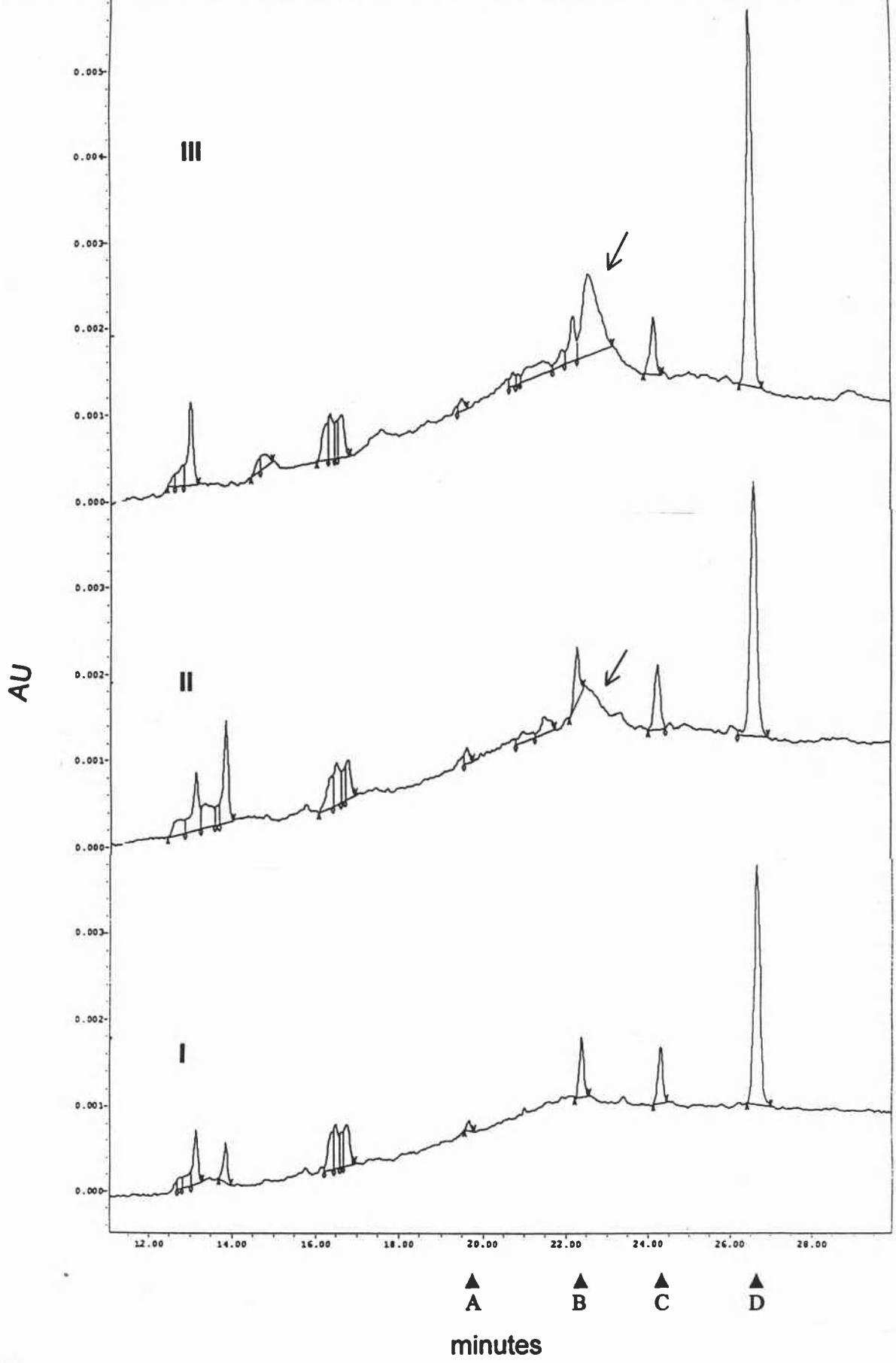

Figure 10: Interference by CHL with DB[*a*,*l*]P metabolite separation on HPLC

Bibliography

1. Reasonably anticipated to be carcinogen: Polycyclic aromatic hydrocarbons, 15 listings. http://ntp-server.niehs.nih.gov/htdocs/ARC/ARC_RAC/PAH.html

2. Jerina, D. M., Yagi, H., Lehr, R. E., Thakker, D. R., Schaffer-Ridder, M., Karle, J. M., Levin, W., Wood, A. W., Chang, R. L. and Conney, A. H. (1978). The bay-region theory of carcinogenesis by polycyclic aromatic hydrocarbons. In *Polycyclic hydrocarbons and cancer vol. 1* (Gelboin, H.V. and Ts'o, P. O., Eds), Academic Press, New York..

3. Levin, W., Wood, A. W., Wislocki, P. G., Chang, R. L., Kapitulnik, J., Mah, H. D., Yagi, H., Jerina, D. M., and Conney, A. H. (1978). Mutagenicity and carcinogenicity of benzo[*a*]pyrene and benzo[*a*]pyrene derivatives. In *Polycyclic hydrocarbons and cancer vol. 1* (Gelboin, H.V. and Ts'o, P. O., Eds), Academic Press, New York.

4. Wood, A. W., Levin, W., Chang, R. L., Lehr, R. E., Schaefer-Ridder, M., Karle, J. M., Jerina, D. M., Conney, A. H. (1977). Tumorigenicity of five dihydrodiols of benz[*a*]anthracene on mouse skin: exceptional activity of benz[*a*]anthracene 3,4-dihydrodiol. *Proc. Natl. Acad. Sci. USA* **74**, 3176-3179.

5. Snook, M. E., Severson, R. F., Arrendale, R. F. Higman, H. C., and Chortyk, O. T. (1977) The identification of high molecular weight polynuclear aromatic hydrocarbons in a biologically active fraction of cigarette smoke condensate. *Beitrag. Tabakforsch.* **9**, 79-101.

6. Lavit-Lamy, D., and Buu-hoi, N. P. (1968) The true nature of 'dibenzo[*a,l*]pyrene and its known derivatives. *J. Chem. Soc. Chem. Commun.*, 92-94.

7. Lacassagne, A., Buu-Hoi, N. P., Zajelda, F., and Vingiello, F. A. (1968) The true dibenzo[*a,l*]pyrene a new potent carcinogen. *Naturwissenschafter* **55**, 43.

8. Higginbotham, S., Ramakrishna, N. V. S., Johansson S. L., Rogan, E. G., and Cavalieri, E. L. (1993) Tumor-initiating activity and carcinogenicity of dibenzo[*a,l*]pyrene versus 7,12-dimethylbenz[*a*]antracene and benzo[*a*]pyrene at low doses in mouse skin. *Cancinogenesis* **14**, 875-878.

9. Cavlieri, E. L., Higginbotham, S., RamaKrishna, N. V. S., Devanesan, P. D., Todorovic, R., Rogan, E. G., and Salmasi, S. (1991) Comparative dose-response tumorigenicity studies of dibenzo[*a,l*]pyrene versus 7,12-dimethylbenz[*a*]anthracene, benzo[*a*]pyrene and two dibenzo[*a,l*]pyrene dihydrodiols in mouse skin and rat mammary gland. *Carcinogenesis* **12**, 1939-1944.

10. Melendez-Colon, V. J., Smith, C. A., Seidel, A., Luch, A., Platt, K. L., and Baird, W. M. (1997). Formation of stable adducts and absence of depurinating DNA adducts in cells and DNA treated with the potent carcinogen dibenzo[*a,l*]pyrene or its diol epoxides. *Proc. Natl. Acad. Sci. USA* **94**, 13542-13547.

11. Devanesan, P. D., Cremonesi, P., Nunally, J. E., Rogan, E. G., and Cavalieri, E. L. (1990). Metabolism and mutagenicity of dibenzo[*a,e*]pyrene and the very potent environmental carcinogen dibenzo[*a,l*]pyrene. *Chem. Res. Toxicol.* **3**, 580-586.

12. Ralston, S. L., Lau, H. H. S., Seidel, A., Luch, A., Platt, K. L., and Baird, W. M. (1994). The potent carincogen dibenzo[*a,l*]pyrene is metabolically activated to fjord regoin 11,12-diol 13,14-epoxides in human mammary carcinoma MCF-7 cell cultures. *Cancer Res.* **54**, 887-890.

13. Shou, M., Krausz, K. W., Gonzalez, F. J., and Gelboin, H. V. (1996). Metabolic activation of the potent carcinogen dibenzo[*a,l*]pyrene by human recombinant cytochromes P450, lung and liver microsomes. *Carcinogenesis* **17**, 2429-2433.

14. Hirayama, T. (1986) Nutrition and cancer – a large scale cohort study. In *Genetic Toxicology of the Diet* (Knudson, I. Ed.) pp 299-311, Alan R. Liss Inc., New York.

15. Hocman, G. (1989) Prevention of cancer: vegetables and plants. *Comp. Biochem. Physiol.* **93B**, 201-202.

16. Trock, B., Lanza, E., and Greenwald, P. (1990). Dietary fiber, vegetables, and colon cancer: Critical review and metaanalyses of the epidemiologic evidence. *J. Natl. Cancer. Inst.* **82**, 650-661.

17. Chernomorsky, S. A., and Segelman, A. B. (1988). Review article: Biological activities of chlorophyll derivatives. *N. Engl. J. Med.* **85**, 669-673.

18. Lam, C. R., and Brush, B. E. (1950). Chlorophyll and wound healing. *Am. J. Surg.* **80**, 204-210.

19. Young, R. W., and Begesi, J. S. (1980). Use of chlorophyllin in the care of geriatric patients. *J. Amer. Geriat. Soc.* **28**, 46-47.

20. Dashwood, R. H., Breinholt, V., and Bailey, G. S. (1991). Chemopreventive properties of chlorophyllin: inhibition of aflatoxin B_1 (AFB_1)-DNA binding in vivo and anti-mutagenic activity against AFB_1 and two heterocyclic amines in the *Salmonella* mutagenicity assay. *Carcinogenesis* **12**, 939-942.

21. Dashwood R. H. (1992). Protection by chlorophyllin against the covalent binding of 2-amino-3-methylimidazo[4,5-f]quinoline (IQ) to rat liver DNA. *Carcinogenesis* **13**, 113-118.

22. Breinholt, V., Hendricks, J., Pereira, C., Arbogast, D., Bailey, G. (1995). Dietary chlorophyllin is a potent inhibitor of aflatoxin B_1 hepatocarcinogenesis in rainbow trout. *Cancer Res.* **55**, 57-62.

23. Park, K-K., and Surh, Y-J. (1996). Chemopreventive activity of chlorophyllin against mouse skin carcinogenesis by benzo[*a*]pyrene and benzo[*a*]pyrene-7,8-dihydrodiol-9,10-epoxide. *Cancer Lett.* **102**, 143-149.

24. Hasegawa, R., Hirose, M., Kato, T., Hagiwara, A., Boonyaphiphat, P., Nagao, M., Ito, N., and Shirai, T. (1995). Inhibitory effect of chlorophyllin on PhIP-induced mammary carcinogenesis in female F344 rats. *Carcinogenesis* **16**, 2243-2246.

25. Guo, D., Horio, D. T., Grove, J. S., and Dashwood, R. H. (1995). Inhibition by chlorophyllin of 2-amino-3-methylimidazo[4,5-*f*]quinoline induced tumorigenesis in the male F344 rat. *Cancer Lett.* **95**, 161-165.

26. Reddy, A., et. al. (1996). *Proc. Am. Assoc. Cancer. Res.* **37**, abs. 276.

27. Dashwood, R. H. and Guo, D. (1992). Inhibition of 2-amino-3-methylimidazo[4,5-*f*]quinoline (IQ)-DNA binding by chlorophyllin: studies of enzyme inhibition and molecular complex formation. *Carcinogenesis* **13**, 1121-1126.

28. Tachino, N., Guo, D., Dashwood, W. M., Yamane, S., Larsen, R., and Dashwood, R. H. (1994). Mechanisms of the in vitro antimutagenic action of chlorophyllin against benzo[*a*]pyrene: Studies

of enzyme inhibition, molecular complex formation and degradation of the ultimate carcinogen. *Mutat. Res.* **308**, 191-203.

29. Breinholt, V., Schimerlik, M., Dashwood, R. H., and Bailey, G. S. (1995). Mechanisms of chlorophyllin anticarcinogenesis against aflatoxin B_1: Complex formation with the carcinogen. *Chem. Res. Toxicol.* **8**, 506-514.

30. Maron, D. M. and Ames, B.N. (1983). Revised methods for the Salmonella mutagenicity test. *Mutation Research* **113**, 173-215.

31. Lowry, O.H., Rosebrough, N. J., Far, A. L., and Randall, R. J., (1951). Protein measurements with the Folin phenol reagent. *J. Biol. Chem.* **193**, 265-275.

32. Burke, M. D., Prough, R. A., and Mayer, R. T. (1977). Characteristics of a microsomal cytochrome P-448-mediated reaction – ethoxyresorufin O-deethylation. *Drug. Metab. Dispos.* **5**, 1-8.

33. Kowalczyk, A, Boens, N., and Ameloot, M. (1997). Determination of ground state dissociation constant by fluorescence spectroscopy. *Meth. Enzymol.* **278**, 94-113.

34. Connors, K. A. (1987) Binding constants – the measurement of molecular complex stability. Wiley Interscience, New York, NY.

35. Dashwood, R. and Guo, D. (1993). Antimutagenic potency of chlorophyllin in the Salmonella assay and its correlation with binding constants of mutagen-inhibitor complexes. *Environ. Mol. Mutagenesis* **22**, 164-171.

36. Lake, B. G. (1987). Preparation and characterisation of microsomal fractions for studies on xenobiotic metabolism. In: Biochemical Toxicology – a practical approach (eds. Snell, K. and Mullock, B.) IRL Press, Oxford. pp 183-215.

37. Berndtson, A. K., and Chen, T. T. (1994). *Arch Biochem. Biophys.* **310**, 187-185.

38. Curtis, L. R., Foster, E. P., La Costa, E. G., Vrolick, N., and Chen, T. T. (1996). *The Toxicologist* **30**, Abs. 379.

39. Ong, T., Whong, W. Z., Stewart, J. D., and Brockman, H. E. (1986). Chlorophyllin: a potent antimutagen against environmental and dietary complex mixtures. *Mutation Res.* **173**, 111-115.

40. Whong, W. Z., Stewart, J. D., Brockman, H. E., and Ong, T. (1988). Comparative antimutagenicity of chlorophyllin and five other agents against aflatoxin B_1-induced reversion of *Salmonella typhimurium* strain TA98. *Teratogen. Carcinogen. Mutagen.* **8**, 215-224.

41. Barnes, W., Tuley, E., and Eisenstadt, E. (1982). Base-sequence analysis of His^+ revertants of the *hisG46* missense mutation in *Salmonella typhimurium*. *Environ. Mutagen.* **4**, 297

42. Ralston, S. L., Seidel, A., Luch, A., Platt, K. L., and Baird, W. M. (1995). Stereoselective activation of dibenzo[a,l]pyrene to (-)-anti(11R,12S,13S,14R)- and (+)-syn(11S,12R,13S,14R)-11,12-diol-13,14-epoxides which bind extensively to deoxyadenosine residues of DNA in the human mammary carcinoma cell line MCF-7. *Carcinogenesis* **16**, 2899-2907.

43. Nesnow, S., Davis, C., Nelson, G., Ross, J. A., Allison, J., Adams, L., and King, L. C. (1997). Comparison of the morphological transforming activities of dibenzo[*a,l*]pyrene and

benzo[*a*]pyrene in C3H10T1/2CL8 cells and characterization of the dibenzo[*a,l*]pyrene-DNA adducts. *Carcinogenesis* **18**, 1973-1978.

44. Prahalad, A. K., Ross, J. A., Nelson, G. B., Roop, B. C., King, L. C., Nesnow, S., and Mass, M. J. (1997). Dibenzo[*a,l*]pyrene-induced DNA adduction, tumorigenicity, and Ki-ras oncogene mutations in strain A/J mouse lung. *Carcinogenesis* **18**, 1955-1963.

45. Cheng, S. C., Hilton, B. D., Roman, J. M., and Dipple, A. (1989). DNA adducts from carcinogenic and noncarcinogenic enantiomers of benzo[*a*]pyrene dihydrodiol epoxide. *Chem. Res. Toxicol.* **2**, 334-340.

46. Sayer, J. M., Chadha, A., Agarwal, S. K., Yeh, H. J. C., Yagi, H., and Jerina, D. M. (1991). Covalent nucleoside adducts of benzo[*a*]pyrene 7,8-diol 9,10-epoxides: Structural reinvestigation and characterization of a novel adenosine adduct on the ribose moiety. *J. Org. Chem.*, **56**, 20-29.

47. Gee, P., Maron, D. M., and Ames, B. N. (1994). Detection and classification of mutagens: a set of base-specific Salmonella tester strains. *Proc. Natl. Acad. Sci. USA* **91**, 11606-11610.